The Journal of Experimental Biology 208, 2103-2114
Published by The Company of Biologists 2005
doi:10.1242/jeb.01603



# Scaling of suction-feeding kinematics and dynamics in the African catfish, *Clarias gariepinus*

Sam Van Wassenbergh*, Peter Aerts and Anthony Herrel

*Department of Biology, University of Antwerp (U.A.), Universiteitsplein 1, B-2610 Antwerpen, Belgium*

*Author for correspondence (e-mail: Sam.VanWassenbergh@ua.ac.be)

*Accepted 15 March 2004*

## Summary

**Scaling effects on the kinematics of suction feeding in fish remain poorly understood, at least partly because of the inconsistency of the results of the existing experimental studies. Suction feeding is mechanically distinct from most other type of movements in that negative pressure inside the buccal cavity is thought to be the most important speed-limiting factor during suction. However, how buccal pressure changes with size and how this influences the speed of buccal expansion is unknown. In this paper, the effects of changes in body size on kinematics of suction feeding are studied in the catfish *Clarias gariepinus*. Video recordings of prey-capturing *C. gariepinus* ranging in total length from 111 to 923 mm were made, from which maximal displacements, velocities and accelerations of several elements of the cranial system were determined. By modelling the observed expanding head of *C. gariepinus* as a series of expanding hollow elliptical cylinders, buccal pressure and power requirement for the expansive phase of prey capture were calculated for an ontogenetic sequence of catfish. We found that angular velocities decrease approximately proportional with increasing cranial size, while linear velocities remain more or less constant. Although a decreasing (angular) speed of buccal expansion with increasing size could be predicted (based on calculations of power requirement and the expected mass-proportional scaling of available muscular power in *C. gariepinus*), the observed drop in (angular) speed during growth exceeds these predictions. The calculated muscle-mass-specific power output decreases significantly with size, suggesting a relatively lower suction effort in the larger catfish compared with the smaller catfish.**

Key words: prey capture, scaling, buccal pressure, dynamic modelling.

## Introduction

Changes in body size have important consequences for the mechanics of musculo-skeletal systems (Hill, 1950; Schmidt-Nielsen, 1984). One of these consequences is that larger animals need more time to carry out the same movement (e.g. downstroke of the wings during flight or leg extension during jumping) compared with smaller animals (Askew et al., 2001; Bullen and McKenzie, 2002; Schilder and Marden, 2004; Toro et al., 2003). Because of the importance of scaling relationships for the ecology, behaviour, performance and evolution of animals (e.g. Carrier et al., 2001; Walter and Carrier, 2002; Hutchinson and Garcia, 2002; Davenport, 2003), theoretical models have been proposed (e.g. Hill, 1950; Richard and Wainwright, 1995). These models provide quantitative predictions of scaling of kinematics in geometrically similar animals.

Although most scaling studies have addressed animal locomotion, several experimental studies have focussed on scaling of prey capture kinematics in aquatic suction feeding vertebrates (Richard and Wainwright, 1995; Reilly, 1995; Cook, 1996; Hernandez, 2000; Wainwright and Shaw, 1999; Robinson and Motta, 2002). Surprisingly, the results of these studies are largely inconsistent. For example, the time to open the mouth increases with body length by $L^{0.592}$ in *Micropterus salmoides* (Wainwright and Shaw, 1999), $L^{0.333}$ in *Gynglymostoma cirratum* (Robinson and Motta, 2002) and $L^{0.314}$ in *Danio rerio* (Hernandez, 2000) and is independent of body size in *Salamandra salamandra* (Reilly, 1995). Furthermore, none of the existing geometrical-similarity models are able to explain the observed results in most cases. Based on the intrinsic dynamics and energetics of contracting muscle, the model of Hill (1950) predicts that similar movements (e.g. a limb rotating a certain angle) should be carried out in times directly proportional to the linear dimensions ($\sim L^1$). On the other hand, the model of Richard and Wainwright (1995) predicts that durations of kinematic events are independent of body size ($\sim L^0$) by assuming that the shortening velocity of a muscle is directly proportional to muscle length (or the number of sarcomeres in series). Consequently, the influence of size on the speed of movements of the feeding system during suction remains a poorly understood phenomenon.

The maximal speed of a given movement is determined by

the equilibrium of forces in the equation of motion for this specific movement. Most of these forces will be subject to size effects. The magnitude of drag force, for example, depends on the surface area of the structures moving through a given fluid and will therefore increase with size. How these external forces scale with animal size, and how this balances with the available muscular power, energy or stress-resistance of bones, will often determine the performance of a given movement (e.g. Hill, 1950; Wakeling et al., 1999).

During the expansive phase of suction feeding, a negative (sub-ambient) pressure is created inside the buccal cavity (see, for example, Van Leeuwen and Muller, 1983; Lauder, 1985). As estimated by Aerts et al. (1987), the force exerted by this negative buccal pressure on the expanding lower jaw is the most important factor to be overcome by the contraction of the mouth-opening muscles. Additionally, a recent study has demonstrated a correlation between the force available from the epaxial musculature and buccal pressure magnitudes in centrarchid fishes (Carroll et al., 2004). This also suggests that intra-buccal pressure is the most constraining factor for the maximal performance of the cranial system of suction feeders. So, if the maximal speed of movements by the cranial musculo-skeletal system during suction is mainly limited by buccal pressure, then scaling effects are probably the results of the size dependency of buccal pressure.

In their theoretical model of suction feeding in fish, Muller et al. (1982) have shown that peak sub-ambient buccal pressure increases drastically (approximately $\sim L^{4.5}$) if an expanding fish head (modelled as an expanding cone) is artificially lengthened without changing the speed of expansion. Therefore, due to scaling effects on buccal pressure, suction feeders may be forced to decrease the speed of buccal expansion when they become larger (resulting in pressure magnitudes that their cranial muscles are capable of generating). Moreover, the existing scaling models (Hill, 1950; Richard and Wainwright, 1995) may not be able to explain scaling of suction-feeding kinematics because the more important effects of changes in pressure with size are not taken into account in these models.

In the present paper, the scaling of prey capture kinematics in the African catfish *Clarias gariepinus* is investigated. Next, the relationships between speed of buccal expansion, cranial size and muscular power requirement are explored by hydrodynamic suction modelling combined with inverse dynamic modelling in *C. gariepinus*. Finally, we evaluate the hypothesis that scaling of suction-feeding kinematics may be determined by the size effects imposed on buccal pressure magnitudes.

## Materials and methods

### *Study animals*

*Clarias gariepinus* (Burchell 1822) is an air-breathing catfish (Fam. Clariidae) with an almost Pan-African distribution that is also found in rivers and lakes of the Middle East and Turkey (Teugels, 1996). It has a broad diet that includes mostly fish, shrimps, crabs, insect nymphs, beetles and snails (Bruton, 1979). While this species shows different kinds of foraging behaviours, including bottom feeding, surface feeding or group hunting, prey are generally captured by a combination of suction feeding and biting (Bruton, 1979; Van Wassenbergh et al., 2004). Juvenile *C. gariepinus* specimens already have a fully ossified cranial system that appears to be generally similar in shape to the adult configuration at the ontogenetic stage of 127 mm standard length (Adriaens and Verraes, 1998). Adults can grow up to 1.5 m total length (Teugels, 1986), making this species particularly suitable for studying scaling effects.

In the present study, we used 17 individuals between 110.8 and 923.0 mm in total length. As the cranial length (defined as the distance between the rostal tip of the premaxilla and the caudal tip of the occipital process) can be measured more precisely and excludes variability in the length of body and tail, we use this metric to quantify size. The individuals used were either aquarium-raised specimens obtained from the Laboratory for Ecology and Aquaculture (Catholic University of Leuven, Belgium) or specimens obtained from aquacultural facilities (Fleuren & Nooijen BV, Someren, The Netherlands). However, catfish from both origins did not show different growth patterns of the feeding apparatus (see Herrel et al., 2005). All animals were kept in a separate aquarium during the course of the training and recording period. In general, it took about two weeks to train the catfish to feed in a restricted part of the aquarium.

### *Video recordings of prey captures*

Video sequences were recorded of *C. gariepinus* capturing pieces of cod (*Gadus morhua*) that were pinned onto a plastic coated steel wire (Fig. 1). In order to obtain a similar feeding situation for both the small and large individuals, the size of the prey was scaled according to the size of the catfish (diameter between 25% and 35% of cranial length). The recordings were made using a Redlake Imaging Motionscope digital high-speed video camera at 250 frames $s^{-1}$ (for individuals with cranial lengths between 28.01 and 71.00 mm), a JVC GR-DVL9800 camera (PAL recording system) at 100 frames $s^{-1}$ (for individuals with cranial lengths of 94.13–130.0 mm) or a Panasonic F15 at 50 frames $s^{-1}$ (for the 210.2 mm cranial length individual). The feeding sequences were recorded simultaneously in lateral and ventral view, using a mirror placed at 45°. Two floodlights (600 W) provided the necessary illumination. Only those prey capture sequences that were approximately perpendicular to the camera lens were selected and retained for further analysis.

### *Kinematic analysis*

Ten recordings were analysed for each individual. Specific anatomical landmarks were digitised using Didge (version 2.2.0, Alistair Cullum, Creighton University, Omaha, NE, USA), from which kinematic variables describing the position of the lower jaw, hyoid, branchiostegal membrane and neurocranium were calculated (see Fig. 2). From kinematic plots, timings of kinematic events (maximum and end of the

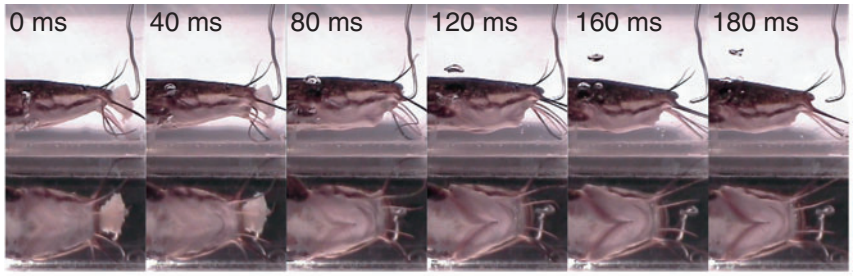


Fig. 1. Selected video frames from a representative prey capture sequence for one individual of *Clarias gariepinus* (30.2 cm total length) feeding on an attached piece of cod. Lateral view (top frames) and ventral view (bottom frames) are recorded simultaneously.

analysed head part movements) were determined, with time 0 being the start of lower jaw depression. After data filtering (4th order Butterworth zero phase-shift low-pass filter) and differentiation *versus* time, velocities and accelerations were calculated. As we are mainly interested in maximal performance, the maximal values per individual (i.e. largest excursions, highest peak velocities and accelerations) were used in the regression analysis. Only for the timing variables were the averages from the 10 analysed sequences for each individual used in the regressions to enable comparison with previous scaling studies (Richard and Wainwright, 1995; Robinson and Motta, 2002).

As growth is an exponential phenomenon, all data were $\log_{10}$-transformed values (one data point for each individual) and were plotted against the $\log_{10}$ of cranial length. Next, least squares linear regressions were performed on these data. As the kinematic variables or the model output (see below; dependent data) probably have a much greater error than measurements of cranial length (independent data), least squares regressions are appropriate in this case (Sokal and Rohlf, 1995). The slopes of these linear regressions (with 95% confidence limits) were determined in order to evaluate changes in prey capture kinematics in relation to changes in body size. A slope of 0 indicates that the variable is independent of cranial length. Slopes of 1 and –1 denote that the variables increase or decrease, respectively, proportional to cranial length, while slopes different from these values stand for a variable changing more than proportionally with cranial length.

Each regression was tested for statistical significance by an analysis of variance (ANOVA). *t*-tests were performed to compare the observed regression slopes against expected values (Zar, 1996). The basic assumptions of normality and linearity were met in the presented data. The significance level of $P$=0.05 was used throughout the analysis.

### *Suction modelling and calculation of buccal pressure*

First, spatio-temporal patterns of water velocities inside the mouth cavity were calculated with the ellipse model of Drost and van den Boogaart (1986). This model has been shown to give accurate predictions of flow velocities in suction-feeding larval carp (*Cyprinus carpio*) (Drost and van Den Boogaart, 1986) and in the snake-necked turtle (*Chelodina longicollis*) (Aerts et al., 2001). This model also gives good predictions of the actual flow velocity for suction feeding of *C. gariepinus*. Results of a high-speed X-ray video analysis of *C. gariepinus* capturing small, spherical pieces of shrimp (6 mm diameter) charged with a small metal marker (0.5 mm diameter) show maximal prey velocities of 1.2 m s$^{-1}$. After applying the suction model (see below for details) to the same individual, the two analysed sequences gave maximal flow velocities of 1.13 and 1.60 m s$^{-1}$ (Van Wassenbergh et al., in press). Assuming that small prey behave approximately as a part of the fluid, these findings suggest that the model output is also realistic for *C. gariepinus*.

In our suction model, the head of the catfish, from mouth aperture to pectoral fin, is approximated by a series of hollow elliptical cylinders (Fig. 3). Each cross-section of this structure

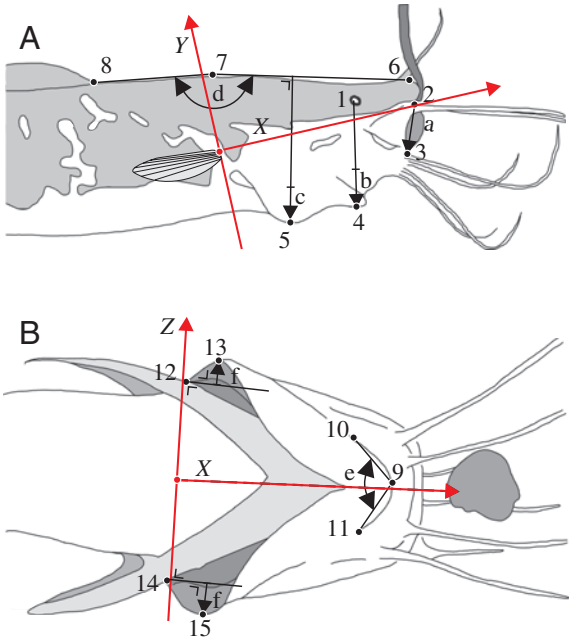


Fig. 2. Anatomical landmarks digitized (black points) with the calculated kinematic variables (arrows) on the lateral (A) and ventral (B) high-speed video images of *Clarias gariepinus*. The landmarks are: 1, middle of the eye; 2, upper jaw tip, interior side; 3, lower jaw tip, interior side; 4, tip of the hyoid; 5, most ventrally positioned point of the branchiostegal membrane; 6, rostral tip of the skull roof; 7, caudal tip of the skull roof; 8, anterior tip of the caudal fin; 9, hyoid symphysis; 10,11, most caudally discernible points on the hyoid bars; 12,14, base of pectoral spine; 13,15, lateral tip of the branchiostegal membrane. The measured linear variables are: gape distance (a), hyoid depression (b), branchiostegal depression (c) and lateral branchiostegal expansion (f, average between left and right). The angular variables are: neurocranial elevation (d) and lateral hyoid abduction (e). The red lines represent the coordinate system moving with the head of the catfish.

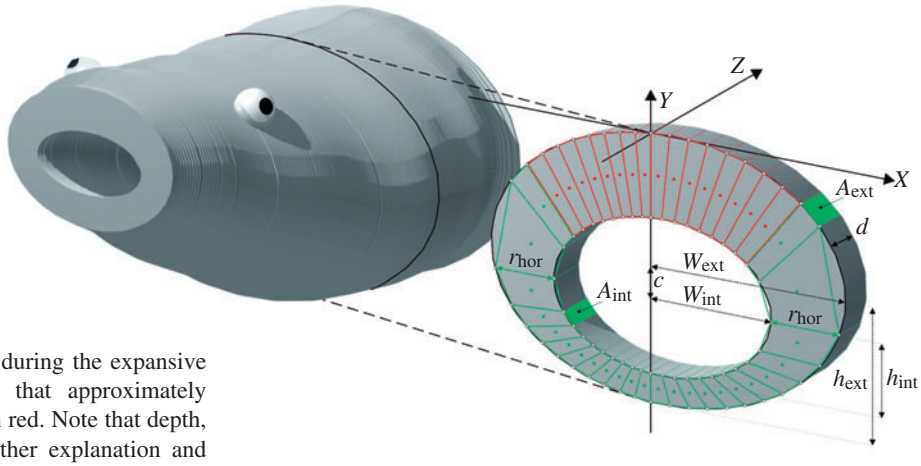


Fig. 3. Three-dimensional representation of the model used for calculation of power requirement of suction feeding in *C. gariepinus*. The model consists of 201 serially arranged hollow elliptical cylinders (left). Each cylinder consists of an external ellipse bordering the fish's head and an internal ellipse bordering the buccal cavity (right). Movement of the centres of mass (red and green dots) of 40 subdivisions of the modelled head volume (red and green segments) with respect to a fixed frame of reference (*XYZ*) was computed during the expansive phase for each cylinder. The 16 segments that approximately correspond to the neurocranium are indicated in red. Note that depth, *d*, is exaggerated for clarity. See text for further explanation and definition of symbols.

consists of an external ellipse and an internal ellipse. The length of the major and minor axis of the external ellipses correspond, respectively, to the height and width of the head at any given position, while the internal ellipse axes approximate the width and height of the bucco-pharyngeal cavity (further referred to as buccal cavity or mouth cavity). Changes in the length of the external ellipse axes were deduced from the recorded videos. To do so, upper and lower contours of the catfish's head were digitised frame by frame (50 points each) in the lateral and ventral view. At the same time, the coordinates of a longitudinal axis connecting the upper jaw tip to a point equidistant between the base of the right and left pectoral fin were digitised (Fig. 2). Next, the contour coordinates were recalculated in a new frame of reference moving with the fish, with the upper jaw tip as origin and the longitudinal axis above as the *X*-axis. The coordinates of each contour curve (upper, lower, left and right contours of the head) were then fitted with $10^{th}$-order polynomial functions, using the XlXtrFun add-in for Microsoft Excel (Advanced System Design and Development, Red Lion, PA, USA). Next, the distance between the corresponding coordinates of the upper and lower contours, and between the left and right contours, were calculated at 201 equally spaced intervals along the longitudinal axis. For each external ellipse, the profiles of length and width *versus* time were filtered with a $4^{th}$-order Butterworth zero phase-shift low-pass filter in order to reduce digitisation noise (cut-off frequency of 30, 12 and 6 Hz for videos recorded at 250 Hz, 100 Hz and 50 Hz, respectively; see above).

The internal dimensions of the mouth cavity of *C. gariepinus* at rest are approximated using X-ray images from lateral and ventral view X-ray videos of a preserved specimen with closed mouth (94.13 mm cranial length; 302.0 mm total length). During recording of these X-ray videos, the specimen was held vertically while a saturated barium solution was poured in the mouth (for illustration, see Van Wassenbergh et al., in press). Using this radio-opaque fluid, the boundaries of the mouth cavity could accurately be distinguished, and the internal area of the mouth cavity determined, for all positions along the longitudinal axis. To account for the presence of the gill apparatus, the length of the major and minor axes of ellipses in the gill region were (arbitrarily) reduced by 10% (see Van Wassenbergh et al., in press). It was assumed that this situation (i.e. the internal volume of the mouth cavity of the preserved specimen at rest) reflects the moment prior to the start of the suction event. Subsequently, changes in the height and the width of the head over time (external ellipses) will cause changes in the width and height of the internal mouth volume ellipses. As internal volume data were collected for one individual only, we are forced to assume that the dimensions of the buccal cavity are proportional to the measured external dimensions of the head in *C. gariepinus*. This means that allometry in the external dimensions of the head is assumed to be reflected in a similar allometry of the bucco-pharyngeal cavity. The X-ray videos were made with a Philips Optimus X-ray generator coupled to a Redlake Imaging MotionPro digital high-speed camera.

According to the continuity principle, any change in volume must be filled instantaneously with water and thus generate a flow relative to the fish's head. So, at each cross-section of the mouth cavity, the total water volume passing through this cross-section in a given amount of time depends on the total volume increase posterior to this cross-section. In this way, the mean flow velocity during a given time increment can be calculated at each of the modelled ellipse-shaped cross-sections of the mouth cavity by dividing the volume increase posterior to this ellipse by the area of the ellipse (average for that time increment). This holds as long as the opercular and branchiostegal valves are closed. If not, the modelled system becomes undetermined (Muller et al., 1982; Muller and Osse, 1984; Drost and van den Boogaart, 1986). In general, branchiostegal valve opening can be detected shortly after *C. gariepinus* reaches maximal oral gape. However, for several of the recorded prey capture sequences, it was problematic to pinpoint precisely the frames in which the transition from closed to opened valves occurred. Therefore, we only used the model output from the start of mouth opening until the time of maximal gape.

Next, pressure inside the expanding modelled profile with closed valves was calculated according to Muller et al. (1982):

$$\frac{\Delta p}{\rho} = \int_x^1 \left[\frac{\partial u}{\partial t} + u\,\frac{\partial u}{\partial x}\right] dx + \left|\frac{u_l'}{(a_r+1)}(x-1) + \frac{u_l}{(a_r+1)}(u-u_l)\right| + \frac{1}{2}\left[\frac{1}{(a_r+1)^2} - 1\right] u_l^2 + \frac{a}{(a_r+1)}(u_l h_l)', \quad (1)$$

where $\Delta p$ is the pressure (difference from hydrostatic pressure), $\rho$ is the density of water (1000 kg m$^{-3}$), $x$ is the position along the longitudinal axis ($x$=0 at the pectoral fin base; $x$=l at the mouth aperture), $u$ is the instantaneous flow velocity of water in x direction, $u_l$ is the instantaneous flow velocity of water in the mouth aperture in a frame of reference moving forward with the head (see Fig. 2), $a_r$ is the ratio between $u_m$ (instantaneous flow velocity of water in the mouth aperture in the earth-bound frame) and ($u_m$–$u_l$), and $h_l$ is the instantaneous radius of the mouth aperture (assumed to correspond to the average between the half width and the half height of the ellipse at this position). The prime sign denotes that the first derivate against time is taken for this function. A representative example of pressures calculated for *C. gariepinus* is shown in Fig. 4.

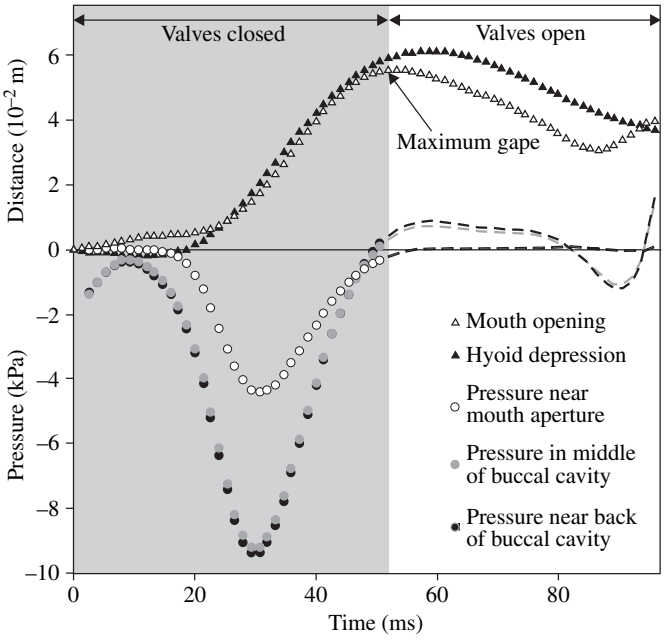


Fig. 4. Example of buccal pressures calculated for a prey capture sequence of a 35.2 mm cranial length *C. gariepinus*. Pressures for three positions inside the buccal cavity (circles), as well as mouth opening (open triangles) and hyoid depression (filled triangles) *versus* time are given. Note that these calculations are only valid when the opercular and branchiostegal valves are closed (grey background) (i.e. approximately until maximal gape is reached).

*Inverse dynamic calculation of required muscular power*

The power required for expanding the series of hollow elliptical cylinders was calculated by inverse dynamics. First, for each hollow cylinder, a new frame of reference is defined with the top of the external ellipse cross-section as the origin, $X$ as the width, $Y$ as the height and $Z$ as the depth (Fig. 3). By doing so, the mid-sagittal part of the skull is entirely motionless in the model, while movement during expansion of the elliptical cylinders will predominantly occur in the ventral and lateral parts of the head. The external ellipses and internal ellipses are now respectively given by the following equations:

$$y = \pm (h_{ext}/w_{ext})\sqrt{w_{ext}^2 - x^2} - h_{ext} \quad (2)$$

$$y = \pm (h_{int}/w_{int})\sqrt{w_{int}^2 - x^2} - h_{ext} - c\,, \quad (3)$$

where $h_{ext}$ and $w_{ext}$ are, respectively, the half height and half width of the external ellipse, $h_{int}$ and $w_{int}$ are, respectively, the half height and half width of the internal ellipse, and $c$ is the distance between the centres of the external and internal ellipses. $c$ was determined from the lateral-view X-ray picture of a 94.13 mm cranial length *C. gariepinus* specimen with a barium-filled buccal cavity and will logically be constant throughout the expansion. The distance from the internal to the external ellipse following the horizontal axis of the internal ellipse ($r_{hor}$) can be calculated by:

$$r_{hor} = \sqrt{(1-c^2/h_{ext})w_{ext}^2} - w_{int}\,. \quad (4)$$

Next, the volume between the internal cylinders and the external cylinders was divided into 40 segments (Fig. 3). To do so, at 20 equally spaced intervals along the horizontal axis of the internal ellipses ($X$-coordinates from $-w_{int}$ to $+w_{int}$) the corresponding $Y$-coordinates were calculated using equation 3. The same was done for the external ellipses ($X$-coordinates from $-w_{ext}$ to $+w_{ext}$) using equation 2. The area between the external and internal ellipse at a given cross-section is now approximated by a series of quadrangles connecting every two adjacent points on the external ellipse with the two corresponding points on the internal ellipse (see Fig. 3). After defining depth, $d$, as the distance between the cross-sections used in the model, we can calculate the volume, the surface area bordering the buccal cavity ($A_{int}$) and the surface area bordering the outside of the fish's head ($A_{ext}$) for each segment (Fig. 3). We assumed that the mass of this volume has the uniform density of 1000 kg m$^{-3}$, which also implies neutral buoyancy. The $xyz$-coordinates of the centre of mass (COM) of any given segment were approximated by taking the average $x$, $y$ and $z$ of the eight corners of the segment.

Thirdly, the linear speed ($v$), acceleration ($a$) and direction of motion of the COM, as well as the inclination of $A_{ext}$ and $A_{int}$, were calculated. As the expansion is symmetrical for the left and right sides of the head, these and the following calculations were performed for a single side. Consequently, final output values (required muscular force; see below) were doubled. Additionally, as the dorsal part of the head (almost static in the model) is taken in by the bony neurocranium, no calculations were performed for this region (see colour scheme in Fig. 3).

To calculate the force required from muscular activity, $F_{muscle}$, the following equation of motion was used:

$$m \cdot a \cdot (1+c_{added}) + F_{pressure} + F_{drag} + F_{muscle} = 0 , \quad (5)$$

where $m$ is the mass, $a$ is the linear acceleration, $c_{added}$ is the added mass coefficient, $F_{pressure}$ is the force resulting from pressure differences between the inside and the outside of the buccal cavity and $F_{drag}$ is the force from hydrodynamic drag. Note that forces resulting from friction between head parts and from deformation of tissues (e.g. stretching of the jaw adductor muscles during mouth opening) are not included. As these forces will probably become important only at the end of cranial expansion, it is assumed that these forces are small compared with the other forces during expansion. The orientation of $F_{pressure}$ is perpendicular to the average inclination of the planes bordering the buccal cavity ($A_{int}$; see Fig. 3) and the outside of the head ($A_{ext}$; see Fig. 3). Its magnitude depends on $\Delta p$ (at a given time and position along the medio-sagittal axis) and surface area. The average surface area of $A_{int}$ and $A_{ext}$ was used for calculating the magnitude of $F_{pressure}$. We used the value of 1 for $c_{added}$ (added mass coefficient for cylinders according to Daniel, 1984), although the importance of changes in this value on the model output will be discussed (see Discussion). $F_{drag}$ is parallel to the direction of motion, and its magnitude was calculated by:

$$F_{drag} = \tfrac{1}{2}\, c_d\, \rho\, A_{ext\text{-}p}\, v^2 , \quad (6)$$

where $c_d$ is the drag coefficient, $\rho$ is the density of water (1000 kg m$^{-3}$), $A_{ext\text{-}p}$ is the area of the external surface of the bar projected onto a plane perpendicular to the direction of motion, and $v$ is the velocity of the COM. A value of 1 was used for the shape-dependent $c_d$, corresponding approximately to drag on an infinite flat plate (Hughes and Brighton, 1999). By using the projected area $A_{ext\text{-}p}$, $F_{drag}$ decreases sinusoidal with the angle of attack of the surface moving through the water, which is in accordance with experimental measurements (Munshi et al., 1999; Bixler and Riewald, 2002).

Finally, total power required from cranial and post-cranial muscles ($P_{req}$) was calculated by:

$$P_{req} = \sum (F_{muscle} \cdot v) . \quad (7)$$

Required power will be expressed as a muscle-mass-specific power by dividing $P_{req}$ (calculated as above) by the mass of a subset of the muscles contributing to the expansions of the cranial system. From all individual catfish used in the present study, the single-sided mass of the protractor hyoidei, sternohyoideus, levator arcus palatini, levator operculi and the part of the hypaxials that is anterior to the pectoral fin basis was measured and summed (Herrel et al., 2005). As this measure of muscle mass is only a fraction of the total mass of the muscles active during the expansive phase of suction feeding (for example, the epaxial muscles are not included), the presented muscle-mass-specific power and mechanical work will overestimate the actual values. They should therefore be regarded as relative, rather than real values. However, we can use these values for analysing the scaling relationships of these variables because it can safely be assumed that the mass of the used sample of muscles will show a similar scaling with cranial size as the total muscle mass contributing to suction.

## Results

### *Linear kinematic variables*

Maximum linear displacements of the lower jaw, hyoid and branchiostegal membrane during prey capture of *C. gariepinus* increase significantly with increasing cranial size (Table 1; Fig. 5A,B). This increase does not differ significantly from a size-proportional increase (slope=1; $P$>0.25). Therefore, no departure from isometry can be distinguished for these variables.

Maximum peak linear velocities of mouth opening, mouth closing, hyoid depression and branchiostegal movements do not change significantly with cranial size (Table 1; Fig. 5C,D). Maximum peak linear accelerations, however, decrease significantly with increasing cranial length (Table 1; Fig. 5E,F). This decrease is almost (and statistically not different from) a decrease proportional to cranial size ($P$>0.07).

### *Angular kinematic variables*

Maximum angular displacements of the neurocranium (elevation) and the hyoid (lateral abduction) do not change significantly with cranial size (Table 1; Fig. 6A,B). This also means that no departure from isometry can be distinguished for these variables.

Maximum peak angular velocities of hyoid abduction and neurocranial elevation decrease significantly with increasing cranial length (Table 1; Fig. 6C,D). In general, this decrease approximates (and is not statistically different from) a decrease proportional to cranial size ($P$>0.13).

### *Timings*

The scaling coefficients (slopes) of timings of the analysed kinematic events are very similar to each other (Table 1). In general, the time from the start of mouth opening until the start, maximum excursion or end of all analysed movements increases approximately proportional to increasing cranial length ($P$>0.29).

### *Buccal pressure*

The magnitudes of peak sub-ambient pressure (i.e. maximal instantaneous pressures averaged over the entire buccal cavity, calculated by the present hydrodynamic modelling) do not change significantly with size (slope=–0.25, $N$=17, $R^2$=0.06, 95% confidence interval between –0.77 and 0.28, $P$=0.337) (Fig. 7A). A similar scaling relationship is found for the magnitudes of the highest (per individual) average buccal pressure (averaged over position and time from start to maximal gape): the linear-regression slope is negative (slope=–0.46, $N$=17, $R^2$=0.21, 95% confidence interval

Table 1. *Scaling relationships for 27 kinematic variables of prey capture in* Clarias gariepinus

| Variable | Slope | $R^2$ | 95% confidence limits | |
|---|---|---|---|---|
| Maximum linear displacements (mm) | | | | |
| Gape distance | 0.912* | 0.87 | 0.715 | 1.109 |
| Hyoid depression | 0.891* | 0.81 | 0.657 | 1.125 |
| Branchiostegal depression | 0.921* | 0.93 | 0.781 | 1.061 |
| Lateral branchiostegal expansion | 0.924* | 0.74 | 0.619 | 1.230 |
| Maximum angular displacements (deg.) | | | | |
| Lateral hyoid abduction | –0.191 | 0.19 | –0.406 | 0.024 |
| Neurocranial elevation | –0.207 | 0.10 | –0.551 | 0.138 |
| Maximum peak linear velocities (mm $s^{-1}$) | | | | |
| Mouth opening velocity | –0.041 | 0.01 | –0.302 | 0.220 |
| Mouth closing velocity | 0.043 | 0.00 | –0.326 | 0.411 |
| Hyoid depression velocity | –0.067 | 0.03 | –0.290 | 0.156 |
| Branchiostegal depression velocity | –0.171 | 0.14 | –0.402 | 0.060 |
| Lateral branchiostegal expansion velocity | 0.223 | 0.09 | –0.173 | 0.618 |
| Maximum peak angular velocities (deg. $s^{-1}$) | | | | |
| Lateral hyoid abduction velocity | –0.951* | 0.83 | –1.186 | –0.716 |
| Neurocranial elevation velocity | –1.223* | 0.84 | –1.519 | –0.926 |
| Maximum peak linear accelerations (mm $s^{-1}$) | | | | |
| Mouth opening acceleration | –0.733* | 0.66 | –1.025 | –0.441 |
| Mouth closing acceleration | –0.779* | 0.67 | –1.077 | –0.480 |
| Hyoid depression acceleration | –0.767* | 0.66 | –1.070 | –0.465 |
| Acceleration of branchiostegal depression | –0.952* | 0.76 | –1.245 | –0.659 |
| Timing variables (s) | | | | |
| Time to maximum gape | 0.927* | 0.91 | 0.771 | 1.082 |
| Time to end of mouth closure | 0.940* | 0.92 | 0.790 | 1.090 |
| Time to maximal hyoid depression | 0.997* | 0.93 | 0.849 | 1.145 |
| Time to end of hyoid elevation | 0.899* | 0.85 | 0.693 | 1.106 |
| Time to maximum branchiostegal depression | 1.068* | 0.92 | 0.900 | 1.236 |
| Time to end of branchiostegal elevation | 1.121* | 0.84 | 0.853 | 1.388 |
| Time to maximum lateral branchiostegal expansion | 0.992* | 0.95 | 0.869 | 1.115 |
| Time to end of lateral branchiostegal expansion | 0.936* | 0.95 | 0.812 | 1.060 |
| Time to maximum lateral hyoid abduction | 1.002* | 0.94 | 0.859 | 1.146 |
| Time to maximum neurocranial elevation | 1.052* | 0.87 | 0.828 | 1.276 |

All variables used in the least squares regressions were $\log_{10}$ transformed. Timing variables are relative to the start of mouth opening (time 0). Slopes differing significantly from 0 at $P<0.05$ (ANOVA) are indicated by *. These slopes were also significant at $P<0.0001$.

between –0.99 and 0.03), although not statistically different from 0 ($P$=0.066) (Fig. 7B).

### *Required power*

The maximal peak power required from the muscular system (calculated by the present hydrodynamic modelling and inverse dynamics) increases significantly ($P$=0.048) with increasing cranial length (slope=0.97, $N$=17, $R^2$=0.24, 95% confidence interval between 0.01 and 1.92). This is also the case for the maximal average power (average from start to maximal gape), which shows a significant ($P$=0.021) increase with increasing size (slope=1.08, $N$=17, $R^2$=0.31, 95% confidence interval between 0.19 and 1.97).

However, when expressed as muscle-mass-specific power (expressed in W $kg^{-1}$ muscle), it also decreases highly significantly ($P<0.0001$) with increasing cranial length (Fig. 8). This is true for the highest (per individual) instantaneous muscle-mass-specific required power (slope=–2.49, $N$=17, $R^2$=0.65, 95% confidence interval between –3.48 and –1.49), as well as for the highest (per individual) average (from start to maximal gape) muscle-mass-specific power (slope=–2.37, $N$=17, $R^2$=0.64, 95% confidence interval between –3.36 and –1.39).

## Discussion

During ontogeny, when *C. gariepinus* becomes larger, important changes in the speed of movements of the cranial structures during suction feeding occur (Figs 5, 6; Table 1). In general, angular velocities decrease approximately proportional with increasing cranial size while linear velocities remain more or less constant (Table 1). These results are not consistent with the previous studies on scaling of suction feeding in vertebrates (Richard and Wainwright, 1995; Reilly,

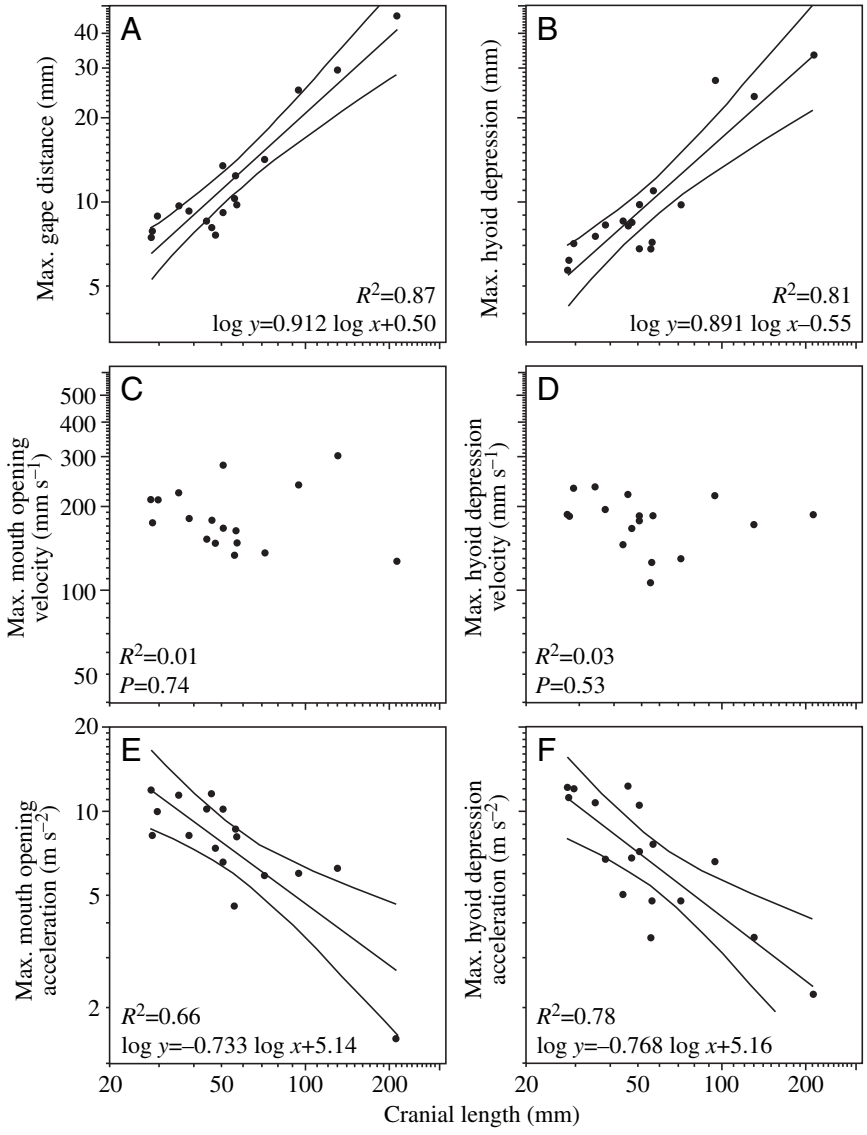


Fig. 5. Log–log plots of maximal linear displacement (A,B), velocity (C,D) and acceleration (E,F) *versus* cranial length, for mouth opening (A,C,E) and hyoid depression (B,D,F).

1995; Hernandez, 2000; Wainwright and Shaw, 1999; Robinson and Motta, 2002). Angular velocity does decrease in these studies but at a lower rate than proportional to body length. Therefore, the results of the present study add to the relatively large interspecific variability in scaling coefficients of aquatic feeding kinematics, which have already been observed among previous studies.

By applying biomechanical modelling to the experimentally observed prey capture kinematics in *C. gariepinus*, a more detailed insight into the mechanics of suction feeding in relation to body size can be achieved. In this way, we may be able to explain the observed scaling relations in prey capture kinematics for this species. In particular, we focus on the potential importance of buccal pressures in limiting the maximal speed of buccal expansions during suction and how this is influenced by size. Results from the model presented in this paper show that the pressure gradient induced by expanding the buccal cavity is theoretically responsible for the largest fraction (>80%) of the total force required from muscular contractions during this expansive phase of suction feeding (Fig. 9). This is in accordance with the findings of Aerts et al. (1987) and Carroll et al. (2004). This also implies that the output of our model (required muscular power) is not very sensitive to changes in the less important factors: inertia (<20% of total required muscular force) and hydrodynamic drag (<2% of total required muscular force). Consequently, the assumptions and approximations that were made in modelling these factors are not critical. For example, tripling the added mass coefficient ($c_{added}$) in the model of a representative prey capture event increases the required power, in general, by less than 3%.

*Scaling relationships predicted by the model*

Assuming that the maximal power output during suction feeding is proportional to the mass of the muscles involved in this process, the presented model can be used to generate specific predictions concerning the scaling of kinematics in *C. gariepinus*. If the linear dimensions of the model are increased isometrically without changing the rate of buccal expansion (i.e. constant angular velocities), the calculated negative buccal pressure magnitudes increase approximately proportional to the square of cranial length (~$CL^2$). As we have shown that sub-ambient buccal pressure is the most important factor in resisting cranial expansion in our model (see above), and given the fact that the surface area of the modelled cranial apparatus to which these pressures apply (~$CL^2$) and linear velocity of expansion (e.g. velocity of the hyoid tip) will also increase in this situation (~$CL$), it was not surprising that our model also shows that power requirement (i.e. required force ~ $CL^4$ multiplied by linear velocity ~ $CL$) increases approximately by $CL^5$. However, the power available from the muscles (i.e. force ~ muscle cross-sectional area multiplied by linear velocity ~ fibre length) only increases by $CL^3$ in the case of isometric growth or by $CL^{3.4}$ if accounting for the positive allometry observed in *C. gariepinus* (Herrel et al., 2005). For this situation, which corresponds to the predictions of the theoretical scaling model of Richard and Wainwright (1995), the required power will exceed the available power during growth. This 'deficit' in power will increase proportional with $CL^2$ (isometry) or with $CL^{1.6}$ (*C. gariepinus* allometry) during growth, forcing *C. gariepinus* to decrease its speed of buccal expansion.

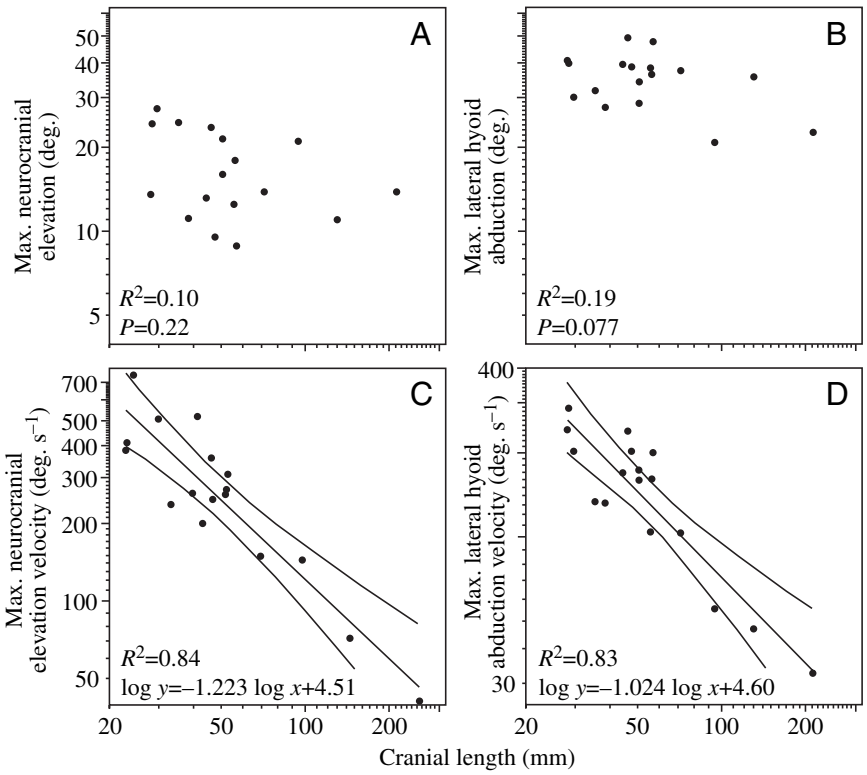


Fig. 6. Log–log plots of maximal angular displacement (A,B) and velocity (C,D) *versus* cranial length for neurocranial elevation (A,C) and lateral hyoid abduction (B,D).

By increasing the time to carry out a given buccal expansion (abbreviated $T$), buccal pressure and power requirement decreases. In order to balance the available and required power, $T$ would have to increase during growth of *C. gariepinus* in a way that the calculated power 'deficit' because of growth ($\sim CL^2$; see above) can be compensated for. By adjusting the expansion time $T$ in our model, we found the buccal pressure changing approximately $\sim T^{-2}$ and power requirement $\sim T^{-3}$. Consequently, in case of isometric growth, equilibrium between the available and required power for buccal expansion is reached when $T$ is increased by $CL^{2/3}$. This corresponds, for example, to angular velocities scaling proportional to $CL^{-2/3}$, and linear velocities scaling with $CL^{1/3}$. Accounting for the positive allometry of muscle mass in *C. gariepinus*, this equilibrium will be reached when the (angular) speed of buccal expansion changes in proportion with $CL^{-1.6/3}$.

However, these theoretical predictions are not confirmed by the experimental data. The observed decrease in the speed of buccal expansion with growth is considerably larger ($\sim CL^{-1}$; Table 1) than the expected scaling relationship ($\sim CL^{-1.6/3}$). In other words, the larger *C. gariepinus* are slower than predicted, or *vice versa*. As a consequence, the model output of muscle-mass-specific power requirement decreases significantly with increasing size (Fig. 8).

### *The model of A. V. Hill*

Scaling relationships found for prey capture kinematics in *C. gariepinus* apparently match the prediction by the scaling model of Hill (1950), in which it was stated that geometrically similar animals should carry out similar movements in times directly proportional to their linear dimensions. In this model, inertial forces (and not hydrodynamic pressures) are assumed to be dominant. If the time to fulfil a given movement does not change with size, then the kinetic energy ($E_k=\frac{1}{2}m\cdot v^2$) required to accelerate a specific mass (for example a limb) scales as length $L^5$ ($m\sim L^3$ and $v^2\sim L^2$). By contrast, the work a muscle can do is expected to increase merely by $L^3$, leaving a 'deficit' in available work increasing by $L^2$. This deficit can be overcome by increasing the time to carry out this movement in proportion to the increasing length, by which the required energy for this movement is in proportion to the total muscle mass.

The forces resulting from buccal pressures calculated for suction feeding in *C. gariepinus* apparently scale similar to the inertial forces outlined by Hill: these forces both increase approximately by $L^4$ in the case of constant speed and by the square of speed in the case of constant size. Consequently, the size and speed dependence of the energetic demands for suction feeding in *C. gariepinus* are expected to be identical to

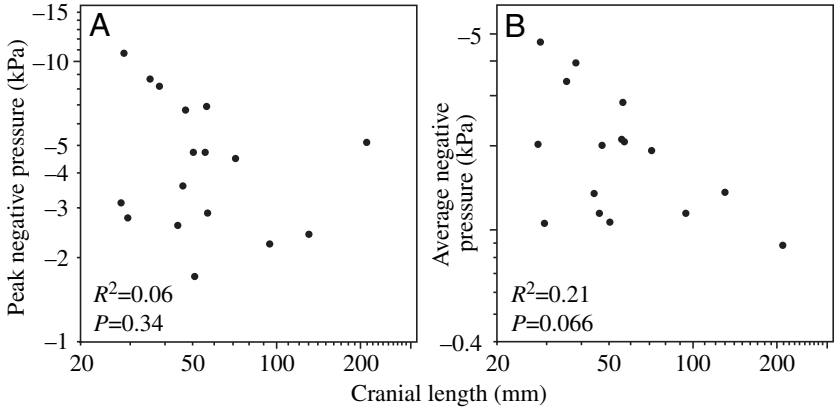


Fig. 7. Log–log plots of maximal peak negative buccal pressure (A) and maximal average buccal pressure (B) *versus* cranial length. These buccal pressures are averaged over the entire buccal cavity (from mouth aperture to pectoral fin) and were calculated with hydrodynamic models (Drost and van den Boogaert, 1986; Muller et al., 1982). Note that no significant changes were found for these pressures in relation to cranial size.

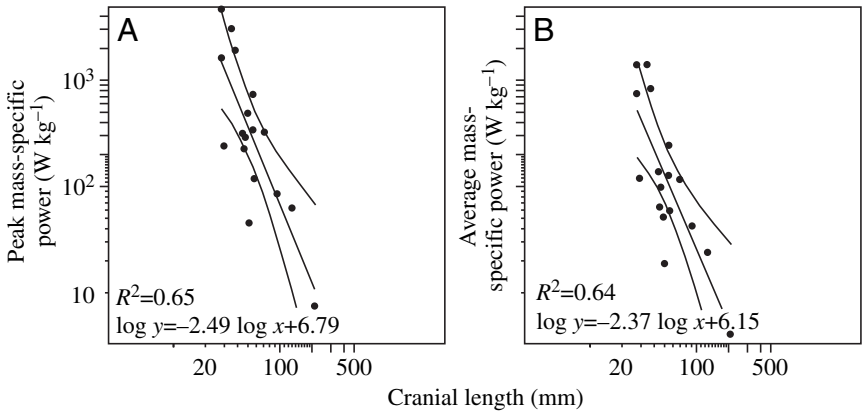


Fig. 8. Log–log plots of peak muscle-mass-specific power requirement (A) and average muscle-mass-specific power requirement (B) *versus* cranial length, as calculated using the model presented in this paper. Note that peak-mass-specific power decreases significantly with increasing cranial size.

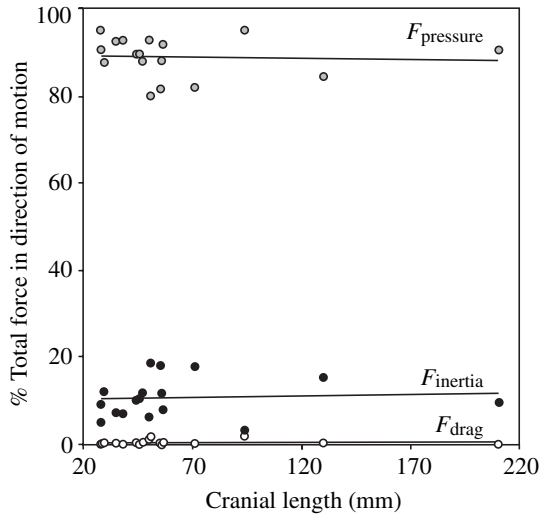


Fig. 9. Relative contribution of forces in the direction of motion as a result of buccal pressure ($F_{pressure}$), acceleration of mass and added mass ($F_{inertia}$) and hydrodynamic drag ($F_{drag}$) to the total force, as estimated by dynamic modelling. Note that forces due to friction between head parts and from deformation of tissues are not included in the model. No significant changes with size are found.

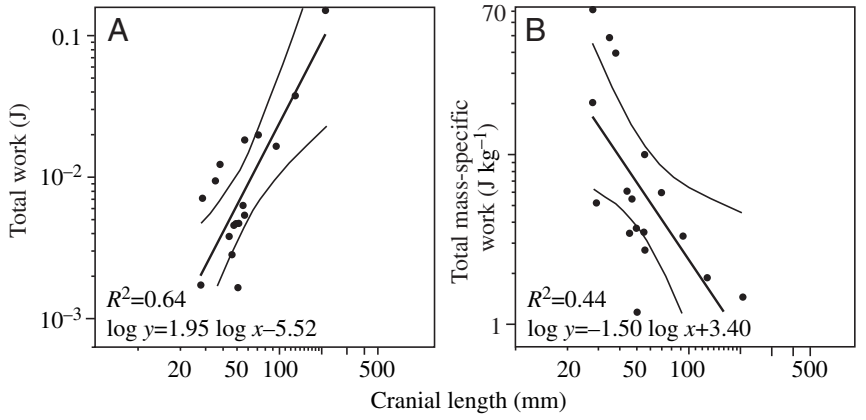


Fig. 10. Log–log plots of total work (A) and muscle-mass-specific work (B) from the start of mouth opening until maximum gape *versus* cranial length, as calculated using the model presented in this paper. Note that, while total work increases significantly with increasing cranial size (A), the muscle-mass-specific work output decreases significantly with increasing cranial size (B).

the acceleration of a limb. Nevertheless, there are still two reasons why this model (Hill, 1950) does not explain the results for *C. gariepinus*. First, one of the assumptions of Hill (1950) is that the muscles are optimized to work at a 'reasonable' energetic efficiency. This assumption does not necessarily apply to occasional, explosive movements such as suction feeding. Furthermore, the mechanical energy or work required for a single suction feeding cycle (which only takes fractions of a second to be completed) is very low compared with the energetic content of prey (Aerts, 1990). For example, if we assume that the total work for buccal expansion in *C. gariepinus* equals twice the work calculated by our model from start to maximum gape, total work is about 0.0034 J for the smallest and 0.3 J for the largest individuals used in this study. On the other hand, the energy content of a small fish prey (1 g wet mass) is approximately 6000 J (Cummins and Wuycheck, 1971). Consequently, as the energetic efficiency of buccal expansion is probably an unimportant aspect of the biology of fishes, we believe that the assumption of the model of Hill (1950), i.e. the size independency of muscle-mass-specific work, is not a good starting point for predicting scaling patterns of an extremely short and anaerobic action such as suction feeding in fish. Note, in this respect, that the maximal power of muscle, $P$, has a different speed dependency than does mechanical work, $E$ ($E=\int P\ \mathrm{d}t$). As a result, different scaling relationships must be predicted if the muscle-mass-specific power instead of muscle-mass-specific work is assumed to be size independent. In the case of suction feeding, maximal power seems a more appropriate speed-limiting factor than muscular energetics (see also Carroll, 2004).

Second, *C. gariepinus* does not fulfil the assumption of geometric similarity. Herrel et al. (2005) measured, for example, a significant positive allometry in the mass (in general approximately $\sim L^{3.4}$) and a negative allometry in the fibre length of the cranial muscles ($\sim L^{0.7}$). As a result, whereas scaling of prey capture kinematics is well predicted by the model of Hill (1950), the size independency of muscle-mass-specific work (an intrinsic assumption of his kinematic predictions) is not observed (Fig. 10).

### *Why are large catfish slower than predicted?*

If we assume that the muscle-mass-specific power output capacity of the muscles involved in buccal expansion does not change with size, the results indicate that larger fish perform sub-maximally compared with smaller fish, in a way that a smaller proportion of the available power is used (Fig. 8). This still leaves us with the question of *why* larger *C. gariepinus* show this apparently reduced suction effort, despite being presented with similar prey of which the size was adjusted according to the size of the catfish. Possibly, faster buccal expansions are not needed for large catfish in order to perform successful prey captures on the experimental prey types. Indeed, it was recently demonstrated for *C. gariepinus* that the actual suction performance (maximal prey distance and size) increases substantially with size, despite the observed decrease in the speed of buccal expansion (Van Wassenbergh et al., in press). For example, it was estimated that the maximal size of a prey that can still be successfully drawn into the mouth by suction increases faster than proportional to cranial size if these prey are sucked from the same absolute distance from the mouth (Van Wassenbergh et al., in press). The observation by Bruton (1979) that larger *C. gariepinus* include a relatively larger amount of evasive prey (i.e. fish) in their natural diet also indicates this increase in suction performance with size. Consequently, the immobile prey of which the size is scaled according to predator size may not have been the ideal situation to induce a comparable suction effort in both small and large *C. gariepinus*. If, as appears to be the case for *C. gariepinus*, some taxa of aquatic suction feeders tend to perform increasingly sub-maximally when becoming larger, this may potentially also explain the large variability observed in the literature on scaling relationships of prey capture kinematics in this group of animals.

### *Conclusions*

Model calculations have shown that negative buccal pressures are responsible for the largest part of the power (more than 80%) required for expanding the buccal cavity during prey capture in *C. gariepinus*. The size dependency of buccal pressures and the forces required for suction feeding will force *C. gariepinus* to become relatively slower during growth; if not, the required power would exceed the expected available power from its muscles (proportional to muscle mass). In this way, we expected *C. gariepinus* to decrease the (angular) speed of movement of its cranial structures during suction proportion to cranial length $CL^{0.53}$. However, the experimental data show that (angular) speed decreases more rapidly with size than predicted: approximately proportional to $CL^{1}$ (Table 1). According to our model, this would imply a significant decrease in the muscle-mass-specific power output. Our data therefore suggest that suction effort employed by the fish to capture similar prey decreases with size. Suction performance, however, does not (Van Wassenbergh et al., in press), leaving the possibility for larger *C. gariepinus* not to use their full muscular capacity while still performing successful prey captures on the experimental prey types we used in this study.

**List of symbols**

| | |
|---|---|
| $a$ | linear acceleration (m $s^{-2}$) |
| $a_r$ | ratio between $u_m$ and ($u_m$–$u_i$) |
| $A_{ext}$ | surface area bordering the outside of the head of a hollow elliptic cylinder segment ($m^2$) |
| $A_{ext\text{-}p}$ | projected area of $A_{ext}$ onto a plane perpendicular to the direction of motion ($m^2$) |
| $A_{int}$ | surface area bordering the buccal cavity of a hollow elliptic cylinder segment ($m^2$) |
| $c$ | distance between the centre of the external and internal ellipses defining the modelled catfish head (m), function of position along the medio-sagittal axis |
| $c_{added}$ | added mass coefficient |
| $c_d$ | drag coefficient |
| $CL$ | cranial length (mm) |
| COM | centre of mass |
| $d$ | distance between two successive points along the medio-sagittal axis for which the cross-section is modelled by ellipses (m) |
| $E$ | mechanical work (J) |
| $E_k$ | kinetic energy |
| $F_{drag}$ | drag force (N) |
| $F_{muscle}$ | muscular force (N) |
| $F_{pressure}$ | force resulting from pressure differences (N) |
| $h_{int}$ | height radius of the internal ellipse (m) |
| $h_{ext}$ | height radius of the external ellipse (m) |
| $h_l$ | radius of the mouth aperture (m) |
| $L$ | body length (mm) |
| $m$ | mass (kg) |
| $P$ | power (W) |
| $P_{req}$ | power required for buccal expansion (W) |
| $\Delta p$ | pressure difference from hydrostatic pressure (Pa) |
| $r_{hor}$ | horizontal distance (left or right) between the internal and external ellipse (m) |
| $t$ | time (s) |
| $T$ | duration of the buccal expansion phase (s) |
| $u$ | flow velocity (moving frame of reference) in the direction of the longitudinal axis (m $s^{-1}$) |
| $u_l$ | flow velocity (moving frame of reference) at the mouth aperture (m $s^{-1}$) |
| $u_m$ | flow velocity at the mouth aperture in earth-bound frame of reference (m $s^{-1}$) |
| $v$ | linear velocity (m $s^{-1}$) |
| $x$ | position along the longitudinal axis |
| $w_{ext}$ | width radius of the external ellipse (m) |
| $w_{int}$ | width radius of the internal ellipse (m) |
| ρ | density (kg $m^{-3}$) |
| ~ | proportional to |

We thank S. Devaere, D. Adriaens, F. Huysentruyt and N. De Schepper for taking care of some of the catfish used in this study. W. Fleuren is acknowledged for supplying *C. gariepinus* specimens. Thanks to F. Ollevier, F. Volckaert and E. Holsters for providing us with *C. gariepinus* larvae and

also the largest individual used in this study. The authors gratefully acknowledge support of the Special Research Fund of the University of Antwerp. A.H. is a postdoctoral fellow of the fund for scientific research – Flanders (FWO-Vl).

## References

**Adriaens, D. and Verraes, W.** (1998). Ontogeny of the osteocranium in the African catfish, *Clarias gariepinus* Burchell (1822) (Siluriformes, Clariidae): ossification sequence as a response to functional demands. *J. Morphol.* **235**, 183-237.

**Aerts, P.** (1990). Variability of the fast suction feeding process in *Astatotilapia elegans* (Teleostei: Cichlidae): a hypothesis of peripheral feedback control. *J. Zool. Lond.* **220**, 653-678.

**Aerts, P., Osse, J. W. M. and Verraes, W.** (1987). Model of jaw depression during feeding in *Astatotilapia elegans* (Teleostei: Cichlidae). Mechanisms for energy storage and triggering. *J. Morphol.* **194**, 85-109.

**Aerts, P., Van Damme, J. and Herrel, A.** (2001). Intrinsic mechanics and control of fast cranio-cervical movements in aquatic feeding turtles. *Am. Zool.* **41**, 1299-1310.

**Askew, G. N., Marsh, R. L. and Ellington, C. P.** (2001). The mechanical power output of the flight muscles of blue-breast quail (*Coturnix chinensis*) during take-off. *J. Exp. Biol.* **204**, 3601-3619.

**Bixler, B. and Riewald, S.** (2002). Analysis of a swimmer's hand and arm in steady flow conditions using computational fluid dynamics. *J. Biomech.* **35**, 713-717.

**Bruton, M. N.** (1979). The food and feeding behaviour of *Clarias gariepinus* (Pisces: Clariidae) in Lake Sibaya, South Africa, with emphasis on its role as a predator of cichlid fishes. *Trans. Zool. Soc. Lond.* **35**, 47-114.

**Bullen, R. D. and McKenzie, N. L.** (2002). Scaling of bat wingbeat frequency and amplitude. *J. Exp. Biol.* **205**, 2615-2626.

**Carrier, D. R., Walter, R. M. and Lee, D. V.** (2001). Influence of rotational inertia on turning performance of theropod dinosaurs: clues from humans with increased rotational inertia. *J. Exp. Biol.* **204**, 3917-3926.

**Carroll, A. M.** (2004). Muscle activation and strain during suction feeding in the largemouth bass *Micropterus salmoides*. *J. Exp. Biol.* **207**, 983-991.

**Carroll, A. M., Wainwright, P. C., Huskey, S. H., Collar, D. C. and Turingan, R. G.** (2004). Morphology predicts suction feeding performance in centrarchid fishes. *J. Exp. Biol.* **207**, 3873-3881.

**Cook, A.** (1996). Ontogeny of feeding morphology and kinematics in juvenile fishes: a case study of the cottid fish *Clinocottus analis*. *J. Exp. Biol.* **199**, 1961-1971.

**Cummins, K. W. and Wuycheck, J. C.** (1971). Caloric equivalents for investigations in ecological energetics. *Int. Assoc. Theor. Appl. Limn.* **18**, 1-158.

**Daniel, T. L.** (1984). Unsteady aspects of aquatic locomotion. *Am. Zool.* **24**, 121-134.

**Davenport, J.** (2003). Allometric constraints on stability and maximum size in flying fishes: implications for their evolution. *J. Fish Biol.* **62**, 455-463.

**Drost, M. R. and van den Boogaart, J. G. M.** (1986). A simple method for measuring the changing volume of small biological objects, illustrated by studies of suction feeding by fish larvae and of shrinkage due to histological fixation. *J. Zool. Lond.* **209**, 239-249.

**Hernandez, L. P.** (2000). Intraspecific scaling of feeding mechanics in an ontogenetic series of zebrafish, *Danio rerio*. *J. Exp. Biol.* **203**, 3033-3043.

**Herrel, A., Van Wassenbergh, S., Wouters, S., Adriaens, D. and Aerts, P.** (2005). A functional morphological approach to the scaling of the feeding system in the African catfish *Clarias gariepinus*. *J. Exp. Biol.* **208**, 2091-2102.

**Hill, A. V.** (1950). The dimensions of animals and their muscular dynamics. *Sci. Prog. Lond.* **38**, 209-230.

**Hughes, W. F. and Brighton, J. A.** (1999). *Schaum's Outline of Theory and Problems of Fluid Dynamics*. Third edition. New York: McGraw-Hill.

**Hutchinson, J. R. and Garcia, M.** (2002). Tyrannosaurus was not a fast runner. *Nature* **415**, 1018-1021.

**Lauder, G. V.** (1985). Aquatic feeding in lower vertebrates. In *Functional Vertebrate Morphology* (ed. M. Hildebrand, D. M. Bramble, K. F. Liem and D. B. Wake), pp. 210-229. Cambridge: The Belknap Press (Harvard University Press).

**Muller, M. and Osse, J. W. M.** (1984). Hydrodynamics of suction feeding in fish. *Trans. Zool. Soc. Lond.* **37**, 51-135.

**Muller, M., Osse, J. W. M. and Verhagen, J. H. G.** (1982). A quantitative hydrodynamic model of suction feeding in fish. *J. Theor. Biol.* **95**, 49-79.

**Munshi, S. R., Modi, V. J. and Yokomizo, T.** (1999). Fluid dynamics of flat plates and rectangular prisms in the presence of moving surface boundary-layer control. *J. Wind Eng. Ind. Aerodyn.* **79**, 37-60.

**Reilly, S. M.** (1995). The ontogeny of aquatic feeding behavior in *Salamandra salamandra*: stereotypy and isometry in feeding kinematics. *J. Exp. Biol.* **198**, 701-708.

**Richard, B. A. and Wainwright, P. C.** (1995). Scaling the feeding mechanism of largemouth bass (*Micropterus salmoides*): kinematics of prey capture. *J. Exp. Biol.* **198**, 419-433.

**Robinson, M. P. and Motta, P. J.** (2002). Patterns of growth and the effects of scale on the feeding kinematics of the nurse shark (*Gynglymostoma cirratum*). *J. Zool. Lond.* **256**, 449-462.

**Schilder, R. J. and Marden, J. H.** (2004). A hierarchical analysis of the scaling of force and power production by dragonfly. *J. Exp. Biol.* **207**, 767-776.

**Schmidt-Nielson, K.** (1984). *Scaling: Why Is Animal Size So Important?* Cambridge: Cambridge University Press.

**Sokal, R. F. and Rohlf, F. J.** (1995). *Biometry*. New York: W. H. Freeman & Co.

**Teugels, G. G.** (1986). Clariidae. In *Checklist of the Fresh-water Fishes of Africa (Cloffa)*, vol. 2 (ed. J. Daget, J. P. Gosse and D. F. E. T. Van Den Audenaerde), pp. 66-101. Brussels, Tervuren, Paris: ISNB, MRAC, ORSTOM.

**Teugels, G. G.** (1996). Taxonomy, phylogeny and biogeography of catfishes (Ostariophysi, Siluroidei): An overview. *Aquat. Living Resour.* **9** (Hors Série), 9-34.

**Toro, E., Herrel, A., Vanhooydonck, B. and Irschick, D. J.** (2003). A biomechanical analysis of intra- and interspecific scaling of jumping and morphology in Caribbean *Anolis* lizards. *J. Exp. Biol.* **206**, 2641-2652.

**Van Leeuwen, J. L. and Muller, M.** (1983). The recording and interpretation of pressures in prey-sucking fish. *Neth. J. Zool.* **33**, 425-475.

**Van Wassenbergh, S., Herrel, A., Adriaens, D. and Aerts, P.** (2004). Effects of jaw adductor hypertrophy on buccal expansions during feeding of air breathing catfishes (Teleostei, Clariidae). *Zoomorphology* **123**, 81-93.

**Van Wassenbergh, S., Aerts, P. and Herrel, A.** (in press). Scaling of suction feeding performance in the catfish *Clarias gariepinus*. *Physiol. Biochem. Zool.*

**Wainwright, P. C. and Shaw, S. S.** (1999). Morphological basis of kinematic diversity in feeding sunfishes. *J. Exp. Biol.* **202**, 3101-3110.

**Wakeling, J. M., Kemp, K. M. and Johnston, I. A.** (1999). The biomechanics of fast-starts during ontogeny in the common carp *Cyprinus carpio*. *J. Exp. Biol.* **202**, 3057-3067.

**Walter, R. M. and Carrier, D. R.** (2002). Scaling of rotational inertia in murine rodents and two species of lizard. *J. Exp. Biol.* **205**, 2135-2141.

**Zar, J. H.** (1996). *Biostatistical Analysis*. London: Prentice-Hall.